Thin Solid Films 519 (2011) 8473–8476

Contents lists available at ScienceDirect

Thin Solid Films

journal homepage: www.elsevier.com/locate/tsf

Metalorganic chemical vapor deposition of β-$FeSi_2$ on β-$FeSi_2$ seed crystals formed on Si substrates

Mitsushi Suzuno [a], Keiichi Akutsu [a], Hideki Kawakami [a], Kensuke Akiyama [b], Takashi Suemasu [a,*]

[a] Institute of Applied Physics, University of Tsukuba, 1-1-1 Tennohdai, Tsukuba, Ibaraki 305-8573, Japan
[b] Kanagawa Industrial Technology Center 705-1 Shimoizumi, Ebina, Kanagawa 243-0435, Japan

ARTICLE INFO

Available online 18 May 2011

Keywords:
β-$FeSi_2$
MBE
MOCVD
Photoresponse
EBSD

ABSTRACT

We have fabricated a β-$FeSi_2$ film by metalorganic chemical vapor deposition on a Si(001) substrate with β-$FeSi_2$ seed crystals grown by molecular beam epitaxy, and investigated the crystallinity, surface morphology and temperature dependence of photoresponse properties of the β-$FeSi_2$ film. The surface of the grown β-$FeSi_2$ film was atomically flat, and step-and-terrace structure was clearly observed. Multi-domain structure of β-$FeSi_2$ whose average size was approximately 200 nm however was revealed. The photoresponse was obtained in an infrared light region (~0.95 eV) at temperatures below 200 K. The external quantum efficiency reached a maximum, being as large as 25% at 100 K when a bias voltage was 2.0 V.

1. Introduction

Semiconducting β-$FeSi_2$ has been attracting much attention as a material for Si-based light emitters and photo detectors (PDs) operating at the optical fiber communication wavelength region since it has been believed to have a direct band gap of 0.83–0.87 eV at room temperature (RT) [1]. Over the past decade, a number of growth methods, such as ion beam synthesis [2], molecular beam epitaxy (MBE) [3,4], and sputtering [5] have been developed for the fabrication of β-$FeSi_2$ films on Si substrates. Metalorganic vapor deposition (MOCVD) is also one of the attractive methods to fabricate β-$FeSi_2$ films [6,7]. Recently, it was reported that β-$FeSi_2$ epitaxial films with a flat surface grown on Si(001) and Si(111) substrates by MOCVD-overgrowth using epitaxial β-$FeSi_2$ seed crystals prepared by reactive deposition epitaxy (RDE), that is Fe deposition on a hot Si substrate [8,9]. Moreover, epitaxial lateral overgrowth of the (100)-oriented β-$FeSi_2$ film by MOCVD from β-$FeSi_2$ seed crystals formed on a Si(001) substrate has been reported [8]. On the other hand, in the case of the (101)/(110)-oriented β-$FeSi_2$ film on Si (111), it has been confirmed that vertical epitaxial growth preferentially occurs from β-$FeSi_2$ seed crystals [9]. This difference was well explained by the fact that β-$FeSi_2$ grows dominantly toward the [101]/[110] direction in MOCVD [8,9].

In this study, we investigate crystallinity, surface morphology, and temperature dependence of photoresponse properties of a β-$FeSi_2$ film grown on a Si(001) substrate by MOCVD-overgrowth with RDE-prepared β-$FeSi_2$ seed crystals.

2. Experimental methods

An ion-pumped MBE system equipped with an electron beam evaporation source for Fe was used to grow β-$FeSi_2$ seed crystals on a Czochralski (CZ) Si(001) substrate. Approximately 20-nm-thick highly (100)-oriented β-$FeSi_2$ epitaxial seed crystals were formed at 470 °C by RDE [10].

For β-$FeSi_2$ deposition on these seed crystals by MOCVD-overgrowth, iron pentacarbonyl [$Fe(CO)_5$] and monosilane [SiH_4] were used as iron and silicon sources, respectively. A liquid $Fe(CO)_5$ source was sealed in a bubbler and carried to the reactor by H_2 gas. The growth rate, total thickness and substrate temperature were 1.33 nm/min, 400 nm and 750 °C, respectively. The operating pressure in the reactor was maintained at 3×10^{-3} Torr. The MOCVD reactor was vertical and cold-well-typed reactor with homemade silicon carbide heater. The Si/Fe atomic ratios of the films were maintained at close to 2 by adjusting the input gas flow rates of the iron and silicon sources, and ratios were cross-checked by X-ray photoelectron spectroscopy (XPS), X-ray fluorescence spectrometry (XRF) and Rutherford backscattering (RBS) using standard samples.

For measuring photoresponse properties, 1.5-mm-spacing striped electrodes were formed with Al on the surface, and sintered at 450 °C for 20 min. The sample was not covered with antireflection coatings.

The crystal quality of the grown layers was characterized by X-ray diffraction (XRD). The observation of surface morphology was carried out by atomic force microscopy (AFM). Electron backscatter diffraction (EBSD) analysis was performed in order to analyze the domain structure of the film. The photocurrent flowing in the lateral direction between the electrodes was evaluated by lock-in technique using a 150 W xenon lamp (1 mW/cm^2 at 1.3–1.6 μm) with a 25-cm-focal-length single monochromator (Bunko Keiki SM-1700A). Light

* Corresponding author.
E-mail address: suemasu@bk.tsukuba.ac.jp (T. Suemasu).

0040-6090/$ – see front matter © 2011 Elsevier B.V. All rights reserved.
doi:10.1016/j.tsf.2011.05.029

intensity was calibrated using a pyroelectric sensor (MELLES GRIOT 13PEM001/J).

3. Results and discussion

Fig. 1 shows θ–2θ XRD patterns of (a) β-$FeSi_2$ seed crystals (before MOCVD-overgrowth) and (b) a β-$FeSi_2$ film after MOCVD-overgrowth. No peaks other than those from the (400), (600) and (800) planes of β-$FeSi_2$ can be observed. This orientation of β-$FeSi_2$ with respect to the Si(001) surface agrees with the epitaxial face relationship between the two materials [11]. The forbidden diffraction peak of Si(200) indicated by * occurs by double diffraction. Fig. 2 shows the surface morphology of β-$FeSi_2$ seed crystals observed by AFM. Approximately 100–200 nm sized high-density nanocrystals can be seen. After MOCVD-overgrowth, flat surface with the RMS roughness of 3.5 nm was obtained as shown in Fig. 3 (a). Moreover, clear step-and-terrace structure was observed. Average step height is approximately 5 Å as shown in Fig. 3 (b), which is half the length of *a* axis of β-$FeSi_2$ unit cell. This step height also corresponds to that observed in the β-$FeSi_2$ bulk [12]. Fig. 4 shows the mapping of the β-$FeSi_2$ crystal planes observed in the β-$FeSi_2$ film after MOCVD-overgrowth by EBSD analysis along the (a) normal (ND) and (b) transverse (TD) directions. The ND and TD mapping show the crystal planes observed in the vertical (β-$FeSi_2$[100]) and lateral (β-$FeSi_2$[010]/[001]) directions of the sample surface, respectively. ND mapping indicates that (100) plane composes a large part of the surface. This result agrees with the θ–2θ XRD patterns shown in Fig. 1 (b). On the other hand, it was found from TD mapping analysis that the blue parts correspond to β-$FeSi_2$ with orientation alignment of β-$FeSi_2$(100)//Si(001) with β-$FeSi_2$[010]//Si[110], while the red parts correspond to that of β-$FeSi_2$(100)//Si(001) with β-$FeSi_2$[001]//Si[110]. The individual domains of β-$FeSi_2$ (100) plane are characterized by either of the two possible 90°-twin orientations. It is noted that the all domains which disagree with the relation of β-$FeSi_2$(100)//Si(001) were designated by black color in the TD mapping to show up this twin. The twining of *a*-axis-oriented β-$FeSi_2$ along the surface normal was also observed by transmission electron microscopy (TEM) [13,14]. Average domain size is on the order of 200 nm. This value corresponds roughly to the size of seed crystals. This result indicates that coalescence of β-$FeSi_2$ domains hardly occur during the MOCVD-overgrowth.

Fig. 5 shows the photoresponse spectra measured under various bias voltages at 100 K for the sample. Light absorption produces electron-hole pairs, which are separated by the electric field between the electrodes, leading to current flow in the external circuit as photoexcited carriers drift before recombination. Photocurrent was

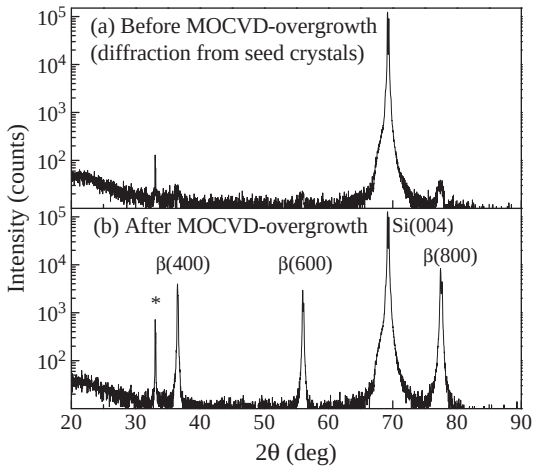

Fig. 1. θ–2θ XRD patterns of (a) β-$FeSi_2$ seed crystals (before MOCVD-overgrowth) and (b) a β-$FeSi_2$ film after MOCVD-overgrowth.

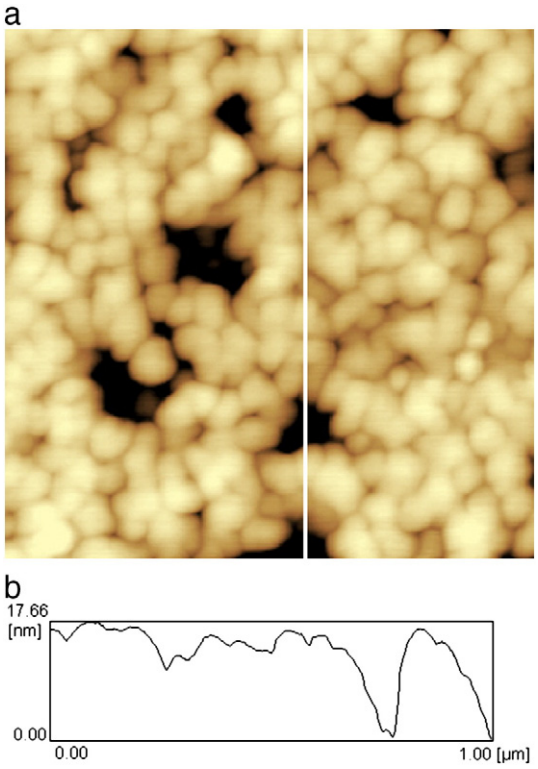

Fig. 2. (a) 1×1 μm^2-area AFM image of β-$FeSi_2$ seed crystals. (b) Cross-section profiles along white line in the AFM image. The upper end of the white line in the AFM image corresponds to 0.00 μm.

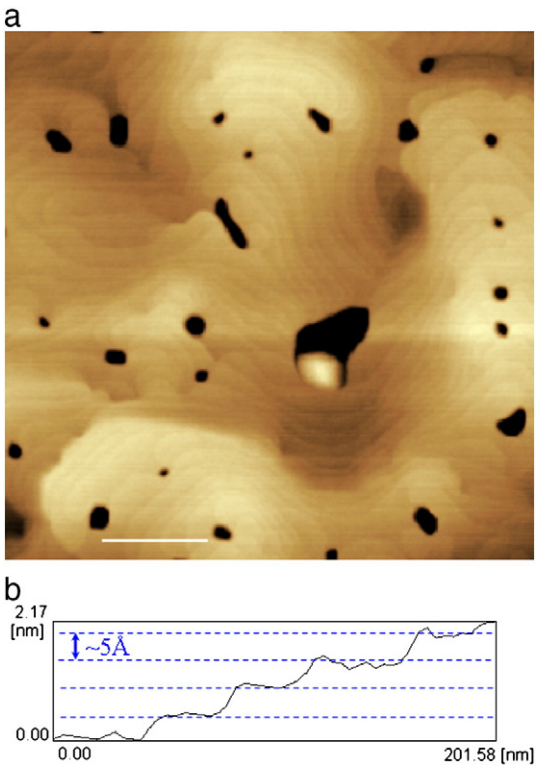

Fig. 3. (a) 1×1 μm^2-area AFM image of a β-$FeSi_2$ film after MOCVD-overgrowth (b) Cross-section profiles along white line in the AFM image. The left end of the white line in the AFM image corresponds to 0.00 μm.

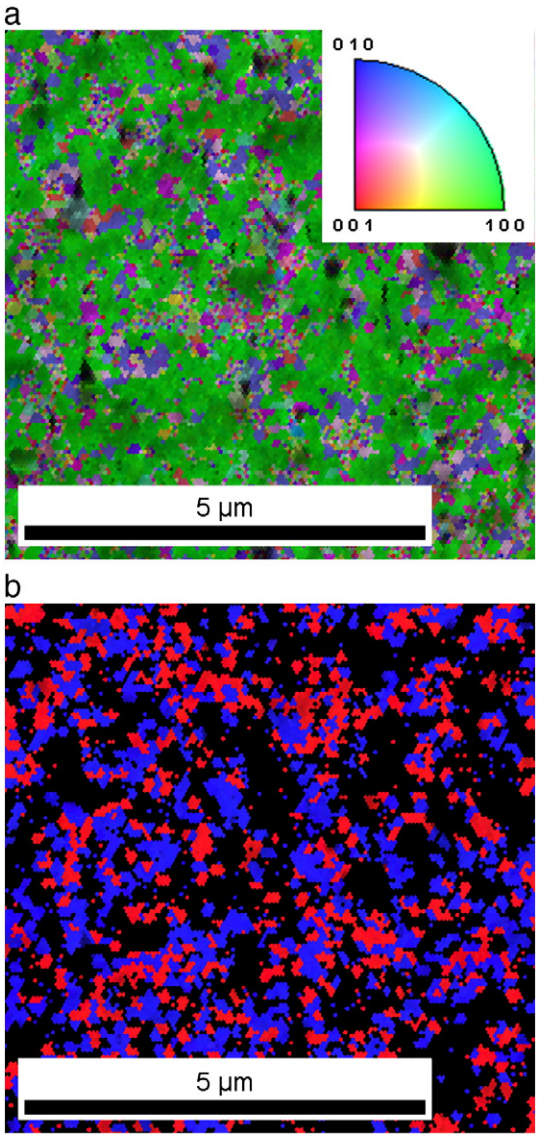

Fig. 4. EBSD mappings observed along the (a) normal (β-$FeSi_2$[100]) and transverse (β-$FeSi_2$[010]/[100]) directions for a β-$FeSi_2$ film.

observed at photon energies greater than 0.8 eV. Photocurrent increases sharply with increasing photon energy, reaching its first peak at approximately 0.95 eV. The second peak is located approximately at 1.55 eV. It is noted that the sharp peaks in photoresponse spectra, such as at 1.45 eV, corresponds to the emission lines of xenon lamp. The photocurrent spectra around the first peak (0.8–1.25 eV) are very similar to the photocurrent spectrum observed for PDs using β-$FeSi_2$ bulk [15,16]. Thus, we assume that the photocurrents around the first peak (0.8–1.25 eV) and the second peak (1.25–3 eV) originate from the contributions of photogenerated carriers in the β-$FeSi_2$ and the Si substrate, respectively. The photocurrent increased linearly with increasing applied bias voltages, and the external quantum efficiency exceeded 25% at 0.95 eV when a bias voltage was 2.0 V. This spectral response is higher by two orders of magnitude than previously-reported spectral response of β-$FeSi_2$ thin films [17]. This is attributed to high-quality β-$FeSi_2$ films grown by MOCVD, as evidence by the clear step-and-terrace structure shown in Fig. 3(b). We don't have enough date to discuss the origin of this photoresponse enhancement at present. Detailed investigations on carrier lifetime or diffusion length of minority carriers will help us understand the mechanism of enhanced photoresponse.

Fig. 6 shows the temperature dependence of photoresponse spectra when a bias voltage was 0.5 V. The photocurrent was observed from the β-$FeSi_2$ at temperatures higher than 20 K. The peak value of photoresponsivity at 0.95 eV increases with increasing temperature, reaching a maximum at 100 K. When the temperature was higher than 100 K, the photoresponsibity decreases sharply with increasing temperature, and then the photoresponse from β-$FeSi_2$ (0.8–1.25 eV) disappeared beyond 150 K. It is not easy to understand these temperature dependences of photoresponsivity, because it is linked to several temperature-dependent rates such as electron-hole recombination rate, the trapping and emission rates of carriers at deep levels, and mobility. However it can be stated at least that electron-hole recombination rate increased with increasing temperature as far as the photocurrent quenching process over 100 K was concerned. This increase in recombination rate might be caused by either increase of residual carrier density or activation of defects working as trap centers of photogenerated carriers, such as grain boundaries shown in Fig. 4 (b) with increasing temperature. Therefore reduction of residual carrier density and defects density must be important to obtain photoresponsivity from β-$FeSi_2$ at room temperature.

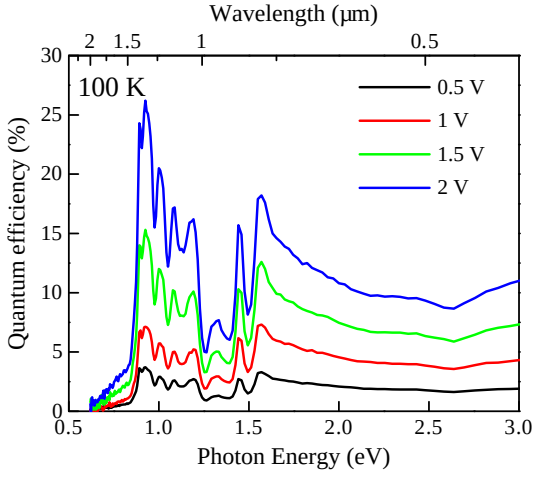

Fig. 5. Photoresponse spectra measured at 100 K for a β-$FeSi_2$ film at various bias voltages between the electrodes.

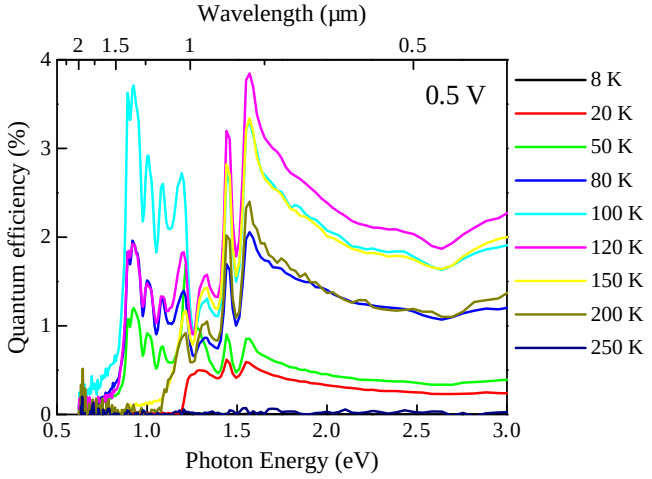

Fig. 6. Photoresponse spectra measured at various temperatures for a β-$FeSi_2$ film at a bias voltage of 0.5 V between the electrodes.

4. Summary

We have fabricated a β-$FeSi_2$ epitaxial film by metal organic chemical vapor deposition on a Si(001) substrate using β-$FeSi_2$ seed crystals grown by molecular beam epitaxy, and investigated crystallinity, surface morphology and temperature dependence of photoresponse properties of the β-$FeSi_2$ film. It was found from AFM observations that 5 Å step-and-terrace structure was clearly seen on the surface of the β-$FeSi_2$ film. EBSD analyses revealed that the average domain size of β-$FeSi_2$ was approximately 200 nm. Clear photoresponse observed at energies ranging from 0.8 to 1.25 eV at temperatures below 200 K was attributed to photogenerated carriers in β-$FeSi_2$. The external quantum efficiency reached a maximum of 25% at 100 K when a bias voltage was 2.0 V.

References

[1] M.C. Bost, J.E. Mahan, J. Appl. Phys. 58 (1985) 2696.
[2] V.E. Borisenko, Semiconducting Silicides, 1st ed Springer-Verlag, Berlin, 2000 Chap. 2.
[3] N. Hiroi, T. Suemasu, K. Takakura, N. Seki, F. Hasegawa, Jpn. J. Appl. Phys. 40 (2001) L1008.
[4] M. Takauji, N. Seki, T. Suemasu, F. Hasegawa, M. Ichida, J. Appl. Phys. 96 (2004) 2561.
[5] T. Yoshitake, Y. Inokuchi, A. Yuri, K. Nagayama, Appl. Phys. Lett. 88 (2006) 182104.
[6] P. Andre, H. Alaoui, A. Deswarte, Y. Zheng, J.F. Petroff, X. Wallart, J.P. Nys, J. Cryst. Growth 144 (1994) 29.
[7] K. Akiyama, S. Ohya, H. Takano, N. Kieda, H. Funakubo, Jpn. J. Appl. Phys. 40 (2001) L460.
[8] K. Akiyama, S. Kaneko, Y. Hirabayashi, T. Suemasu, H. Funakubo, J. Cryst. Growth 287 (2006) 694.
[9] K. Akiyama, Y. Hirabayashi, S. Kaneko, T. Kimura, S. Yokoyama, H. Funakubo, J. Cryst. Growth 289 (2006) 37.
[10] M. Tanaka, Y. Kumagai, T. Suemasu, F. Hasegawa, Jpn. J. Appl. Phys. 36 (1997) 3620.
[11] J.E. Mahan, V.L. Thanh, J. Chevrier, I. Berbezier, J. Derrien, R.G. Long, J. Appl. Phys. 74 (1993) 1747.
[12] Y. Yamada, I. Wakaya, S. Ohuchi, H. Yamamoto, H. Asaoka, S. Shamoto, H. Udono, Surf. Sci. 602 (2008) 3066.
[13] H.-U. Nissen, E. Mumller, H.R. Deller, H. Von Kanel, Phys. Status Solidi A 150 (1995) 395.
[14] Y. Ozawa, T. Ohtsuka, Cheng Li, T. Suemasu, F. Hasegawa, J. Appl. Phys. 95 (2004) 5483.
[15] T. Ootsuka, T. Suemasu, J. Chen, T. Sekiguchi, Appl. Phys. Lett. 92 (2008) 042117.
[16] T. Ootsuka, T. Suemasu, J. Chen, T. Sekiguchi, Y. Hara, Appl. Phys. Lett. 92 (2008) 192114.
[17] Z. Liu, M. Osamura, T. Ootsuka, S. Wang, Y. Fukuzawa, Y. Suzuki, R. Kuroda, T. Mise, N. Otogawa, Y. Nakayama, H. Tanoue, Y. Makita, Opt. Mater. 27 (2005) 942.